Tropical Aquatic and Soil Pollution

Research Article
Volume 5(2), 2026, 110–124
https://doi.org/10.53623/tasp.v5i2.775

Land Degradation Detection in Urban Areas Using Spatial Modelling and Semi-Automatic Classification of Satellite Imagery Data

Riska Ayu Purnamasari[1]*, Marwan Setiawan[2], Wardah Wardah[2]

[1]Department of Soil Science, Faculty of Agriculture, Universitas Gadjah Mada, Jalan Flora, Bulaksumur, Yogyakarta 55281, Indonesia
[2]Research Center for Ecology and Ethnobiology, National Research and Innovation Agency (BRIN), Indonesia Jl. Raya Jakarta Bogor Km. 46, Cibinong, Bogor Regency, West Java 16911, Indonesia

*Correspondence: riska.ayupurnamasari@ugm.ac.id

SUBMITTED: 21 July 2025; REVISED: 14 August 2025; ACCEPTED: 18 August 2025

ABSTRACT: Urban land degradation poses a growing challenge in rapidly developing countries like Indonesia, where population growth and limited space drive uncontrolled land cover changes. This study aims to detect land degradation in urban areas through spatial modelling and semi-automatic classification of multi-temporal remote sensing imagery. Landsat-5 Thematic Mapper (TM) image from year 2011 and Landsat-9 Operational Land Imager collection 2 (OLI-2) image from year 2023 data were acquired from the The United States Geological Survey (USGS). Image pre-processing included band stacking, subsetting, and enhancement to improve visual interpretation. Semi-automatic supervised classification was applied to map seven land cover classes: agricultural dry land, rice field, forest, plantation, non-agricultural land, water body, and settlement. Training data and validation were supported by Google Earth Pro, official sources, and field surveys using random sampling. Change detection analysis revealed a 1664.65 ha increase in industrial areas, accompanied by significant reductions in rice fields (−1726.92 ha) and dry farmland (−1644.57 ha). The classification accuracy reached 80.24% and 75.11%, with kappa coefficients of 0.76 and 0.65, respectively. Results indicate that urban expansion is a key driver of land degradation, particularly through the loss of productive agricultural land. This research demonstrates the effectiveness of remote sensing-based spatial modelling and classification techniques for monitoring urban land degradation and informing sustainable land use planning.

KEYWORDS: Agricultural land; land degradation; landsat imagery; remote sensing; semi-automatic classification

1. Introduction

Increased competition for land use between the agricultural and non-agricultural sectors was a major driver of land degradation in urban areas. The expansion of industrial zones, roads, and other infrastructure led to the large-scale conversion of productive agricultural land, particularly in rapidly urbanizing regions [1, 2]. Industrialization, followed by accelerated

urban growth and population increase, emerged as the dominant cause of agricultural land loss [3, 4]. The development of new industries attracted migration, which resulted in population concentration and the repurposing of land for settlement [5]. This urban expansion not only reduced the extent of arable land but also accelerated environmental degradation, disrupted the ecological balance, and contributed to the decline in soil quality and land productivity. These changes posed significant challenges to food security and sustainable land use in urban environments [6–8]. The continued conversion of agricultural land to urban use resulted in both direct and indirect forms of land degradation, threatening the long-term sustainability of urban ecosystems and the resilience of food systems [9, 10]. In this context, land degradation was defined as the long-term reduction in land productivity and ecological function, detectable through declines in vegetation cover, increases in bare soil, and shifts in land cover classes toward less productive states. Land degradation involved a general decline in cropland's ability to provide ecosystem goods and services. In our analysis, degradation was detected using Landsat-derived classification results, where persistent transitions from vegetated to barren or degraded classes over the study period were identified as indicators of degradation [10]. Monitoring and detecting these changes were therefore critical for effective spatial planning and land degradation mitigation in urban landscapes.

Indonesia underwent rapid urbanization, with the urban population increasing from 22.3% in 1980 to 56.7% in 2020, and projected to reach 63.4% by 2030. Cilegon City in Banten Province, known as the gate of Java Island, was a region with a developing economy, a dense population, and fast urbanization [11]. The urbanization rate increased by about 2.44 times in 10 years, clearly exceeding the national average. While urban growth drove economic and social development, it also placed considerable pressure on natural resources and degraded critical ecological services [12, 13]. Cilegon City, in particular, underwent significant land cover transformations, including the widespread conversion of cropland, forests, and wetlands into residential and industrial zones. Past studies documented these changes, such as land use analysis in the Banten Bay coastal area and land cover change in Cilegon from 1992 to 2003 [14], both of which highlighted significant ecological disruption due to rapid urban expansion. However, the city still lacked comprehensive and accurate land cover change detection systems. Conventional monitoring methods, which relied on manual surveys and descriptive analysis, were time-consuming, costly, and limited in spatial and temporal accuracy. These limitations highlighted the critical need for advanced spatial modelling and remote sensing techniques to effectively detect and assess land degradation in urban environments like Cilegon.

Remote sensing technologies became increasingly essential for monitoring urban growth and its impacts on environmental sustainability. Satellite imagery provided timely, accurate data on land cover dynamics, including the conversion of agricultural land into urban areas [15]. This information enabled policymakers and planners to identify areas at risk of land degradation and to develop strategic interventions for preserving agricultural zones. Remote sensing supported informed decision-making in sustainable land use planning, helping to maintain ecological balance [16]. Over the past two decades, remote sensing applications expanded significantly, with various models and techniques developed to monitor land cover changes and detect environmental degradation [11, 12]. The integration of spectral reflectance data allowed scientists to assess urban expansion and land transformation with increasing precision [17, 18]. Furthermore, satellite imagery and diverse sensor technologies were widely

used to monitor vegetation indices, crop conditions, and ecosystem health across different landscapes [18]. These advancements showed the potential of remote sensing and spatial modelling in detecting land degradation and supporting sustainable urban development. Advancements in image processing and classification techniques using remote sensing significantly enhanced land cover mapping and the detection of land cover changes [23]. Land cover maps were critical for various applications, including land use policy formulation, agricultural monitoring, urban planning, nature conservation, and ecosystem assessment. Land cover classification was typically conducted using satellite imagery and supervised classification techniques that relied on user-defined training data to distinguish among land cover types [23, 24]. Recent studies applied semi-automatic classification based on the random forest algorithm to improve efficiency and reproducibility in land cover classification [25, 26]. These tools offered functionalities such as radiometric correction, post-classification accuracy assessment, and change detection analysis [26].

The aims of this research were to classify land cover types, assess the extent of agricultural land conversion, and detect signs of land degradation caused by urban expansion utilizing semi-automatic classification based on the random forest algorithm applied to Landsat-5 Thematic Mapper (TM) and Landsat-9 Operational Land Imager Collection 2 (OLI-2) satellites. The accuracy of the classification results was evaluated using ground truth data, official land use sources, and statistical metrics such as overall accuracy and the Kappa coefficient. A key novelty of this study lay in its integration of open-source, semi-automatic classification tools with spatial modelling to provide an accessible and cost-effective method for monitoring urban land degradation.

2. Methodology

2.1.Study area.

Based on its geographical location, the City of Cilegon was situated at the far western end of Java Island, lying between 5º52’24”–6º04’07” South and 105º54’05”–106º05’11” East. Administratively, the boundaries of the City of Cilegon were as follows: the north, east, and south sides bordered Serang Regency, while the west side bordered the Sunda Strait. The city consisted of coastal areas in the north and west, rural areas in the south, and urban areas in the north and the city center. The urban areas were equipped with infrastructure facilities that supported socioeconomic development, while residential areas were concentrated in the city center (Figure 1).

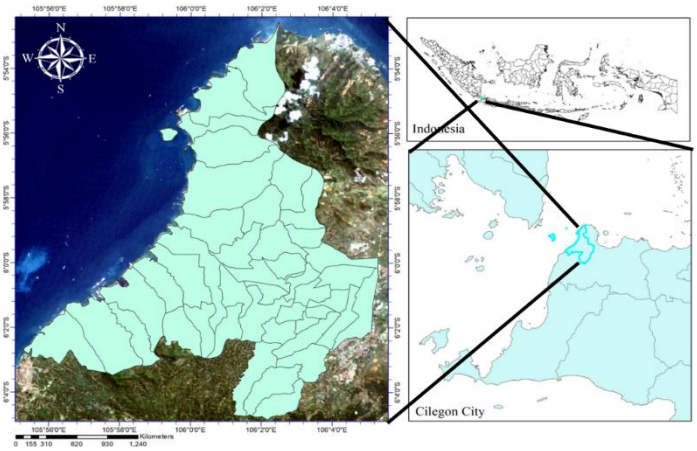

Figure 1. The study area in Cilegon City, Banten Province, Indonesia.

2.2. Framework of the research.

Two sets of land cover map classifications were carried out for two different years (2011 and 2023) using Landsat satellite imagery. The satellite data were sourced from the United States Geological Survey (USGS) website, which provides open access to users. The images were acquired in the same season to ensure comparability. Despite the twelve-year gap, this approach ensured that vegetation and agricultural conditions were similar. Images from Landsat-5 TM and Landsat-9 OLI-2 were selected for analysis. The satellite images were processed using the open-source software QGIS 3.22, which included atmospheric correction and sub-setting of the study area. A false-color composite representation of the multispectral imagery was then used to identify land cover classes (Figure 2). Supervised classification methods, specifically semi-automated classification based on the random forest algorithm, were applied for land cover classification. Accuracy assessments were performed on both images to evaluate classification performance. When the accuracy evaluation results were acceptable, the generated maps were used to detect post-classification changes.

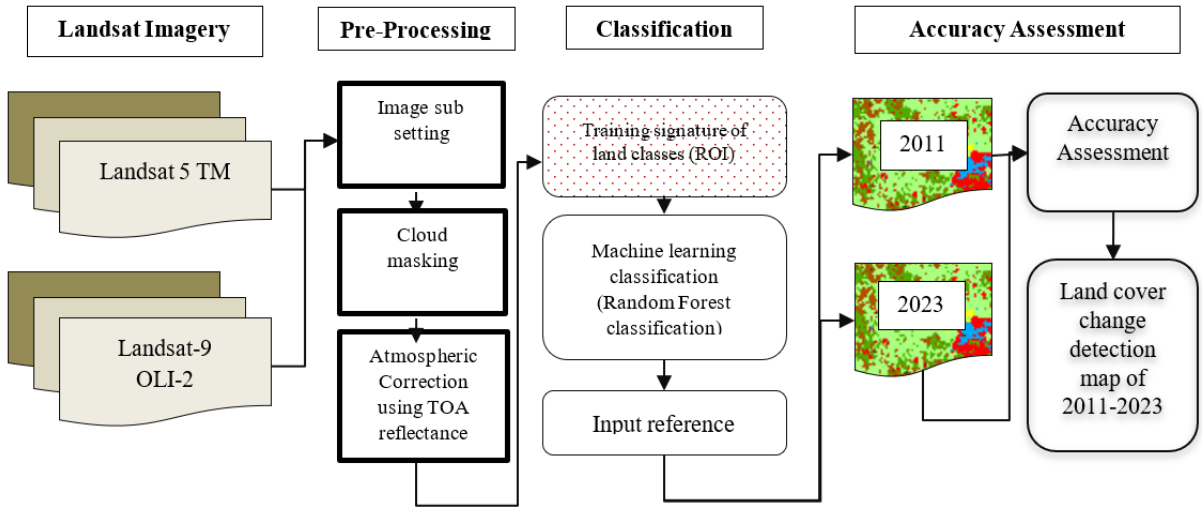

Figure 2. Framework of the research.

2.3. Data pre-processing.

Images from Landsat-5 TM and Landsat-9 OLI-2 were selected for analysis. The available Landsat-5 TM and Landsat-9 OLI-2 data for the study region were used. Based on the mission timeline of each Landsat sensor, Landsat-5 TM recorded images on 8 June 2011, and Landsat-9 OLI-2 recorded images on 19 July 2023. The images were selected from the same season to ensure comparable vegetation conditions. Landsat-5 TM and Landsat-9 OLI-2 had a spatial resolution of 30 m with seven and eleven spectral bands, respectively (Table 1).

Table 1. Remote sensing datasets.

Satellite Images	Sensors	Mission Timeline	Acquired Time
Landsat 5	Thematic Mapper (TM)	March 1984- January 2013	8th June 2011
Landsat 9	Operational Land Imager-Colletion 2 (OLI-2)	September 2021-Till Date	19th July 2023

The satellite images were processed using the open-source software Quantum Geographic Information System (QGIS) 3.22. The preprocessing included atmospheric correction and sub-setting of the study area. An accuracy assessment was performed to evaluate land classification performance. Landsat Level-2 files were directly downloaded from the United States Geological Survey (USGS). The Digital Number (DN) values from the original satellite data were converted into Top-of-Atmosphere (TOA) reflectance values. The preprocessing involved converting DN to radiance, and subsequently radiance to TOA reflectance, for both Landsat-5 TM (Table 2) and Landsat-9 OLI-2 (Table 3). Atmospheric correction was then conducted by converting TOA reflectance to surface reflectance in QGIS. Radiometric calibration and dark object subtraction methods were applied to minimize atmospheric scattering effects, thereby improving the accuracy and comparability of multi-temporal classification results. This process assumed that certain pixels in the imagery had near-zero reflectance; the apparent reflectance of these dark objects was attributed to atmospheric path radiance, which was then subtracted from all pixels. This adjustment enhanced comparability between multi-temporal datasets and improved land cover classification accuracy. Following preprocessing, supervised classification was performed using the Semi-Automatic

Table 2. Spatial and spectral resolution of Landsat 5 TM.

Bands	Wavelength (micro-meters)	Resolution (meters)
Band 1 - Blue	0.45-0.52	30
Band 2 - Green	0.52-0.60	30
Band 3 - Red	0.63-0.69	30
Band 4 - Near Infrared (NIR)	0.76-0.90	30
Band 5 - Shortwave Infrared (SWIR) 1	1.55-1.75	30
Band 6 - Thermal	10.40-12.50	120* (30)
Band 7 - Shortwave Infrared (SWIR) 2	2.08-2.35	30

Table 3. Spatial and spectral resolution of Landsat 9 OLI-2.

Bands	Wavelength (micro-meters)	Resolution (meters)
Band 1 - Ultra Blue (coastal/aerosol)	0.435 - 0.451	30
Band 2 - Blue	0.452 - 0.512	30
Band 3 - Green	0.532 - 0.589	30
Band 4 - Red	0.636 - 0.672	30
Band 5 - Near Infrared (NIR)	0.850- 0.879	30
Band 6 - Shortwave Infrared (SWIR) 1	1.565 - 1.651	30
Band 7 - Shortwave Infrared (SWIR) 2	2.105 - 2.294	30
Band 8 - Panchromatic	0.503 - 0.676	15
Band 9 - Cirrus	1.363 - 1.384	30
Band 10 - Thermal Infrared (TIRS) 1	10.60 - 11.19	100
Band 11 - Thermal Infrared (TIRS) 2	11.50 - 12.51	100

Classification Plugin (SCP) in QGIS, based on the Random Forest (RF) algorithm. RF, a machine learning ensemble method known for its robustness and high classification accuracy under diverse conditions [38], was applied to the processed imagery. Training samples (regions of interest, ROIs) were created for seven land cover classes: rice fields, dryland agriculture, forests, plantations, urban areas, water bodies, and non-agricultural land (Table 4). ROIs were digitized using three different false-color composite schemes to enhance class separability. Training samples (signatures) serving as ROIs were prepared using these composite channel

combinations before supervised classification was conducted (Figure 3). To identify land cover objects, the study applied three distinct false-color composite schemes.

Table 4. Description of land cover classes.

No	Class Name	Description home
1	Rice field	Agriculture field specific for paddy plant
2	Agriculture dry field	Greenhouses, horticulture farms, and other
3	Forest	Forests with open canopies, including green open space and urban forest
4	Plantation	Agriculture crops other than rice
5	Urban area	Human settlement and transportation infrastructure, as well as industrial infrastructure
6	Water bodies	Continental water surfaces (lake, water, dam, and river)
7	Non-agricultural land	Areas devoid of any vegetation cover and characterized by exposed rocks.

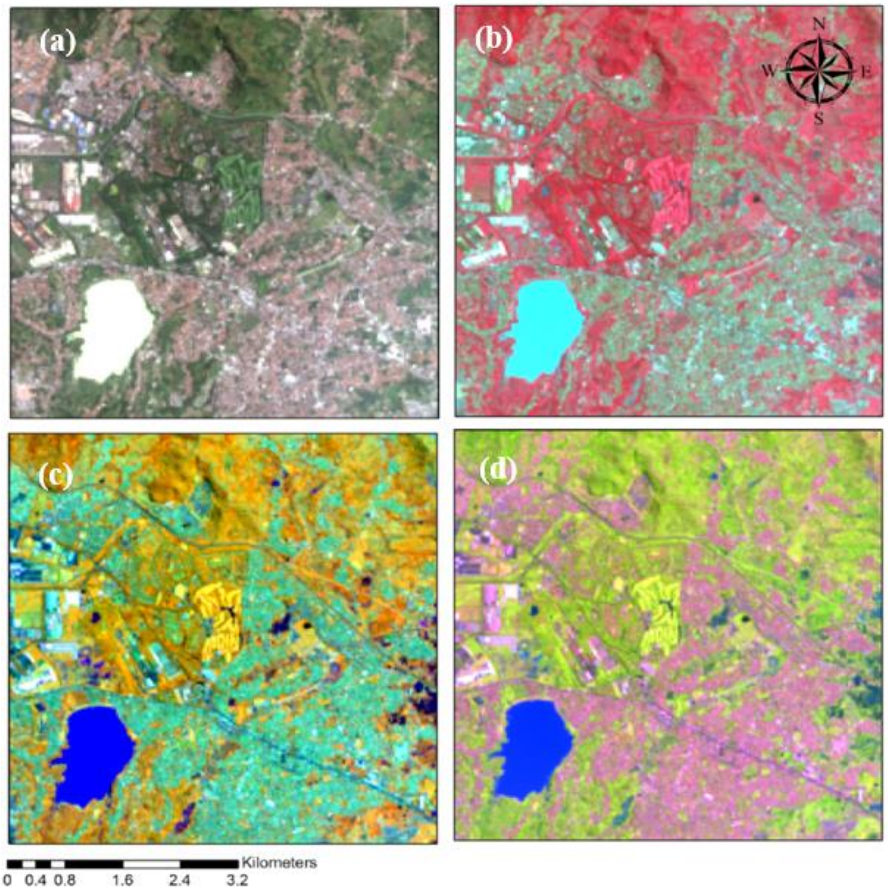

Figure 3. Different colour composites of Landsat-9 OLI-2 images used to create a ROI of different land classes as training samples: a. Natural Color, b. RGB = 5-4-3 c. RGB = 5-6-4, d. RGB = 6-5-4.

2.4. Spatial modelling on raster-based classification.

In this study, spatial modelling was performed through raster-based classification using machine learning, specifically the Random Forest (RF) algorithm. Landsat imagery was pre-processed into reflectance bands and ancillary indices, which were then used as inputs for supervised learning to classify land cover. Each pixel was treated as an observation, with predictor variables derived from spectral bands and calculated indices. The classification model followed a decision-tree-based approach. The RF algorithm was an ensemble learning method that predicted outcomes by integrating multiple decision trees to perform classification [24,

25]. It effectively handled high-dimensional data, accommodated missing values, and reduced overfitting. It was widely applied in various domains, including remote sensing and image classification in QGIS. The RF classifier combined predictions from many decision trees to assign a class label to each pixel. Each decision tree was trained on a fraction of the training data, with bootstrap samples selected randomly, and only a subset of the available features considered at each split [26]. This approach made the RF classifier versatile, robust, and well-suited for handling mixed pixels and complex land cover patterns.

2.5. Land cover change.

Land cover change between 2011 and 2023 was calculated using the following equation (L):

$$L = \frac{U_b - U_a}{U_a} \; x \; \frac{1}{T} \; x \; 100\% \qquad (1)$$

where U_a is the area (ha) of a particular land class at the beginning, U_b is the area (ha) of the land class at the end, and T is the period of analysis. This equation calculated the rate of land cover change between the two survey years. Multiplication by 100% expressed the change as a percentage. Land cover change detection was then performed using the post-classification change detection tool in ArcGIS®. Data on total land cover change and unchanged areas between 2011 and 2023 were compiled into a land cover change detection map for the period 2011–2023.

2.6. Accuracy assessment of land cover classification.

Accuracy evaluation of classification maps was an essential step for validating the classified images. Accuracy assessments were conducted for the 2011 and 2023 classified images to determine the reliability of the derived information. A stratified random sampling method was used to compare the reference images with the classified images at randomly selected points. A total of 252 points served as reference data for the accuracy evaluation, and classification accuracy was quantified using the nonparametric kappa test. Independent validation datasets were also inspected for each period. The accuracy of classification was calculated using a confusion matrix with common statistical measures: producer accuracy (PA), user accuracy (UA), overall accuracy (OA), and kappa statistics. Area-specific accuracy was further quantified by adjusting the estimated land cover area based on classification error ratios [39]. The stratified evaluation method also enabled quantification of area estimation uncertainty based on the 95% confidence intervals associated with each class.

3. Result

The accuracy assessment of the classified land cover maps was carried out through comparison with reference data. The reference data were generated using a combination of random sample points, field identification, and imagery from Google Earth Pro (Figure 4). Ground truth data obtained from these sources were then used to validate the classification results. An overall accuracy evaluation for Cilegon City was conducted using the random forest classification method, as summarized in Tables 5–6.

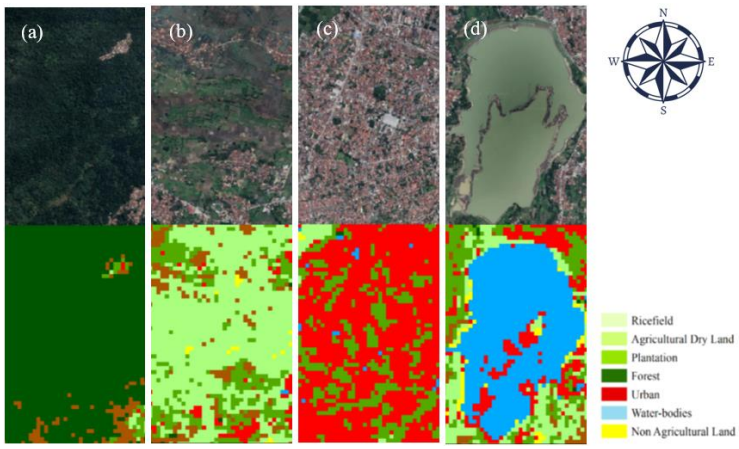

Figure 4. Reference map from ©2023 Google 2023: (a) forest, (b) rice field, (c) settlement, (d) waterbody.

Table 5. Confusion matrix of the land cover 2011 for random forest classifier.

	Land Cover	References							
		RF	**AD**	**PL**	**FR**	**UR**	**WB**	**NA**	**Total**
Classified	Rice field (RF)	49	1	1	0	0	0	17	68
	Agriculture dry land (AD)	6	12	0	0	0	0	1	19
	Plantation (PL)	6	1	43	0	0	0	0	50
	Forest (FR)	0	4	19	1227	0	0	0	1250
	Urban (UR)	0	3	0	0	36	3	4	46
	Waterbodies (WB)	0	0	0	0	0	80	0	80
	Nonagricultural land (NA)	10	0	0	2	0	9	14	35
	Total	**71**	**21**	**63**	**1229**	**36**	**92**	**36**	**1548**

Overall Classification Accuracy = **83.15%,** Overall Kappa Statistics = **0.76.**

Table 6. Confusion matrix of the land cover 2023 for random forest classifier.

	Land Cover	References							
		RF	**AD**	**PL**	**FR**	**UR**	**WB**	**NA**	**Total**
Classified	Rice field (RF)	18	12	0	31	9	0	15	82
	Agriculture dry land (AD)	18	16	4	11	18	0	15	82
	Plantation (PL)	29	4	72	16	0	0	2	123
	Forest (FR)	20	1	15	1324	1	0	48	1409
	Urban (UR)	4	0	0	0	127	0	26	157
	Waterbodies (WB)	0	0	0	0	0	70	0	70
	Nonagricultural land (NA)	73	27	6	16	4	0	56	182
	Total	**162**	**60**	**97**	**1398**	**159**	**70**	**162**	**2108**

Overall Classification Accuracy = **80.41%,** Overall Kappa Statistics = **0.63.**

Visual representations of the classified land cover for 2011 and 2023 are shown in Figure 5. In 2011, the spatial pattern was dominated by agricultural land and rice fields. By contrast, the 2023 data indicated a marked increase in urbanization within Cilegon City. Specifically, non-agricultural land increased by 60.08% and urban areas expanded by 3.70%, while rice fields, dry agricultural land, and plantations decreased by 3.12%, 0.90%, and 2.36%, respectively (Figure 6). A graphical comparison further emphasized the decline in rice fields and the surge in urbanization between 2011 and 2023 (Figure 7). The land cover change classification revealed that urban areas expanded by approximately 1276.73 hectares between 2011 and 2023. Over the same period, rice fields decreased by 1181.36 hectares and dry agricultural land by 365.81 hectares. Conversely, non-agricultural land increased substantially by 1664.65 hectares (60.08%) (Table 7). These changes suggested that land previously used

for agriculture was increasingly converted for other purposes, including commercial and industrial development.

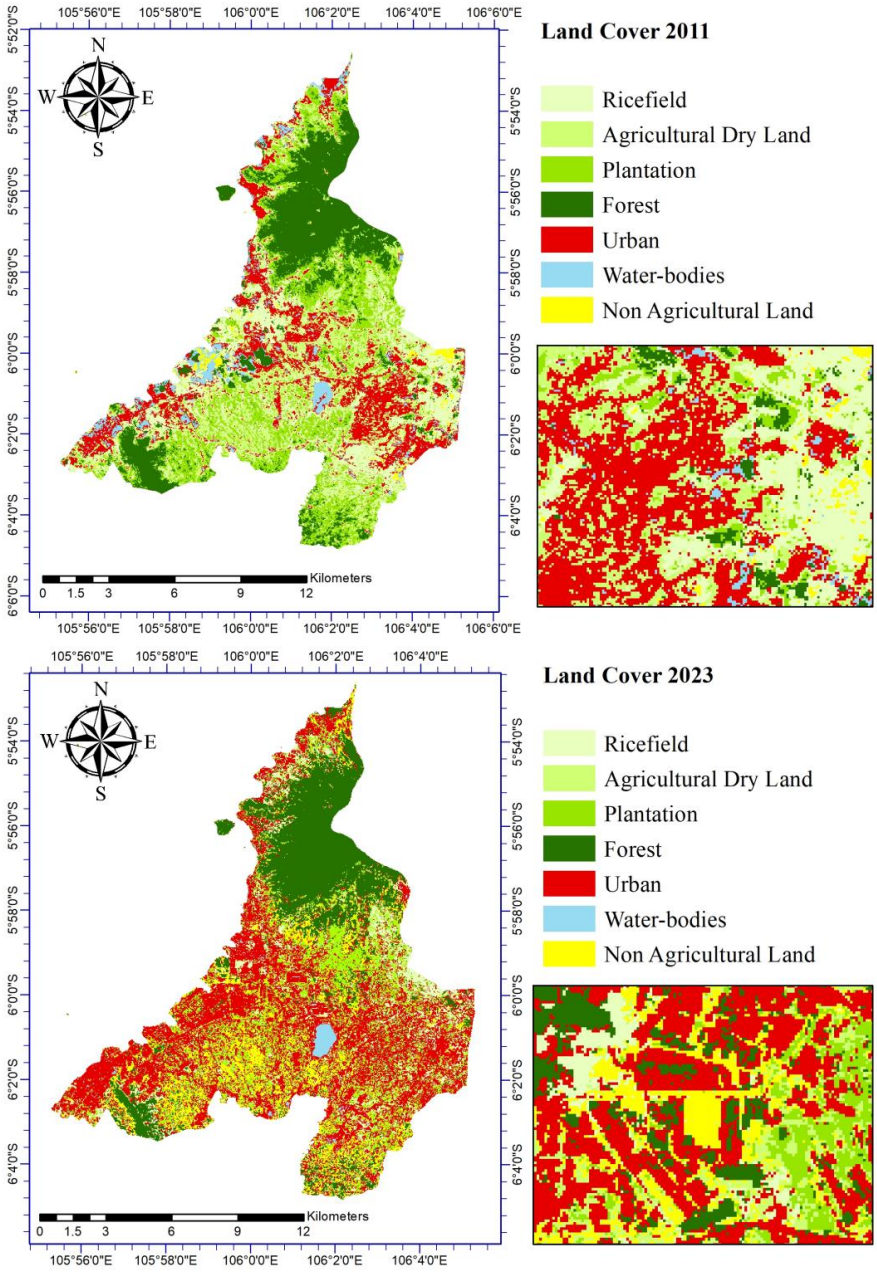

Figure 5. Land cover change map in Cilegon city using random forest classifier.

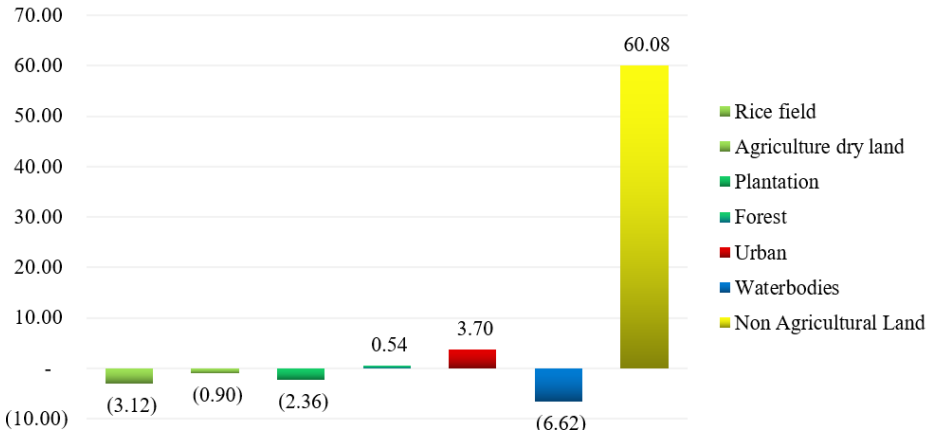

Figure 6. Land cover change rate (RS) RF-based land cover.

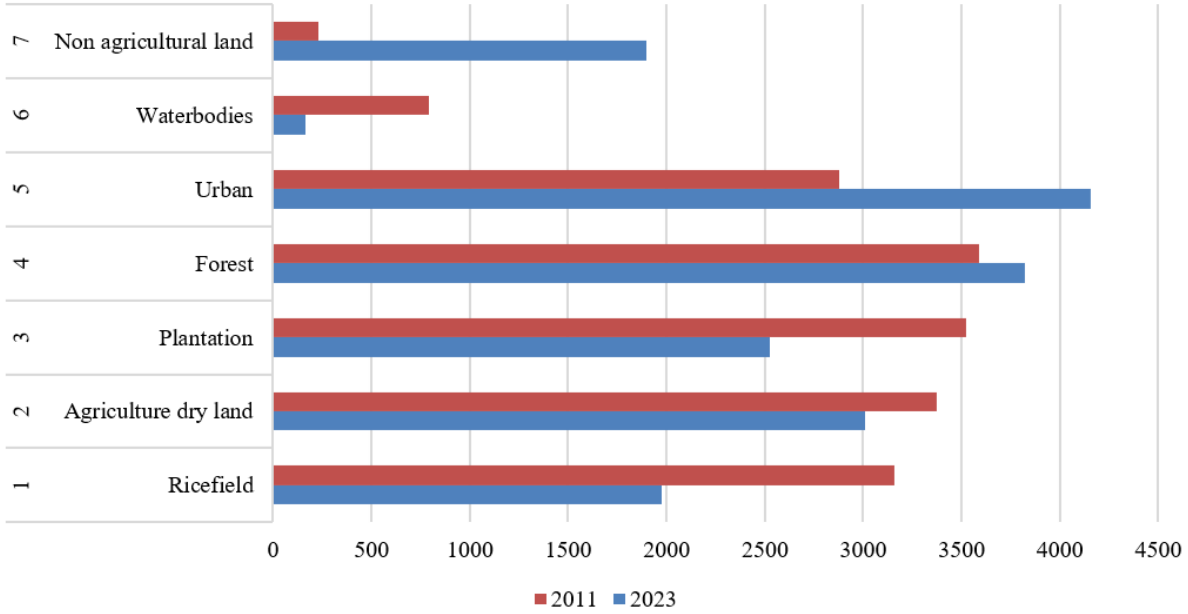

Figure 7. Land cover change data RF-based land cover.

Table 7. Results of the land cover classification of 2011 and 2023.

LULC	2011		2023		Land cover change (ha)	Land cover change rate (%)
	Area (km^2)	Area (ha)	Area (km^2)	Area (ha)		
Rice field	31.60	3159.71	19.78	1978.35	-1,181.36	-3.12
Agriculture Dry Land	33.73	3373.01	30.07	3007.20	-365.81	-0.90
Plantation	35.24	3524.20	25.26	2526.03	-998.17	-2.36
Forest	35.88	3588.07	38.22	3822.34	234.27	0.54
Urban	28.78	2878.43	41.55	4155.16	1,276.73	3.70
Waterbodies	7.93	793.44	1.63	163.12	-630.32	-6.62
Non-Agricultural Land	2.31	230.88	18.95	1895.53	1,664.65	60.08

4. Discussion

This study demonstrated the effectiveness of semi-automatic classification techniques in detecting land degradation and monitoring land cover change in urban areas. By utilizing multi-temporal datasets from Landsat-5 TM and Landsat-9 OLI-2, we mapped and assessed the spatial dynamics of land cover change in Cilegon City between 2011 and 2023. The classification models performed reliably for both years, with higher accuracy observed in the 2011 dataset, possibly due to clearer spectral separation among land cover classes during that period. A key finding of this study was the significant decline in agricultural land, particularly rice fields, dryland agriculture, and plantations, over the twelve-year period. This decline reflected an alarming trend of urban expansion encroaching upon fertile agricultural areas. The transformation of these productive lands into built-up areas not only threatened food security but also undermined the ecological functions provided by these landscapes [28]. These findings supported growing concerns over the vulnerability of peri-urban agricultural zones to urban sprawl. We observed a notable increase in non-agricultural land and urban settlements, highlighting a shift toward land allocated for infrastructure, industrial use, sand mining, and other non-agricultural functions. This trend was strongly correlated with demographic and economic drivers, including population growth, migration for employment, and industrial

development. The strategic location of Cilegon as a gateway to Java, combined with its proximity to Jakarta, intensified these pressures and accelerated land conversion in lowland and coastal areas traditionally used for seasonal agriculture.

Interestingly, forest cover also expanded during the study period, signifying a positive trend toward the preservation and growth of vegetated areas. This increase may have resulted from active reforestation efforts or governmental policies promoting ecosystem restoration. The Cilegon Environment Agency reported similar increases in forest and vegetation areas, likely linked to the Regional Plan of Cilegon City, which mandated that at least 30% of the total area be maintained as green open space. This highlighted the importance of land-use policy in managing urban ecological sustainability. The findings emphasized the value of satellite-based land cover analysis for urban environmental monitoring. Remote sensing provided a rapid, cost-effective, and scalable approach for detecting land use changes, especially in regions experiencing rapid urban transformation. When integrated into spatial models, these data supported policy development and decision-making aimed at mitigating land degradation and preserving ecosystem services.

In coastal cities like Cilegon, urbanization posed unique risks due to the ecological sensitivity of coastal zones. Conversion of coastal land to urban use led to biodiversity loss, increased surface runoff, pollution, and disruption of coastal ecosystems. The loss of agricultural land observed in this study had direct implications for land degradation. Conversion of cropland to barren or degraded land often caused declines in soil organic matter and nutrient availability, leading to chemical degradation. The removal of vegetation exposed soils to wind and water erosion, accelerating physical degradation. Furthermore, replacing diverse agricultural systems with less productive or non-vegetated surfaces reduced habitat availability and ecosystem services, contributing to ecological decline. These impacts were exacerbated by climate change and sea-level rise, underscoring the urgency of sustainable urban planning strategies. Approaches such as green infrastructure, coastal zone management, and smart growth principles should therefore be prioritized to balance development needs with environmental integrity. When compared with previous studies, our findings aligned with research by Gandharum et al. [29], who reported rapid agricultural land degradation in peri-urban areas of West Java driven by industrial expansion. Similarly, Gandharum et al. [30] documented that urban growth in coastal Indonesian cities often targeted productive agricultural land due to accessibility and flat terrain. However, our study demonstrated that integrating multi-temporal Landsat imagery with semi-automatic classification in QGIS provided greater spatial detail than earlier manual methods. This approach captured subtle land cover transitions, including secondary vegetation growth and small-scale reclamation projects. Such findings underscored the importance of open-source tools and free satellite datasets for producing robust, reproducible monitoring frameworks to guide sustainable land management. Overall, the spatial modelling and remote sensing-based land cover analysis presented in this study provided a valuable tool for detecting land degradation and guiding sustainable urban development. The framework was replicable for other rapidly urbanizing regions and contributed to the growing body of knowledge on land system science and sustainable land management.

5. Conclusion

Understanding classification processes was crucial for effectively monitoring land cover change. Geospatial analysis of land cover dynamics played an important role in monitoring systems, enabling the detection of long-term changes that are vital for sustainable land management. Land cover change and urban expansion posed significant risks to food security and environmental protection, but the application of satellite remote sensing in land-use monitoring provided an opportunity to inform and reform policy, particularly at the local government level. In this study, a decision support system was developed using Landsat-5 TM and Landsat-9 OLI-2 datasets. The use of semi-automatic classification tools ensured high accuracy in land-use management and decision-making. Designed to be user-friendly, this approach required only basic GIS knowledge, making it accessible to local governments and non-specialists. Pre-processing could be conducted with open-source software such as QGIS, increasing its applicability. The method was reliable, repeatable, and suitable for use at local, regional, and national levels. However, limitations were noted in moderate-resolution imagery such as Landsat, particularly in heterogeneous urban areas where mixed pixels were common. Features smaller than a single pixel could not be effectively detected, posing challenges for fine-scale monitoring. Future research should incorporate higher-resolution satellite datasets and advanced machine learning techniques to overcome these limitations. The proposed integrated decision-making model could be recommended to Indonesian policy planners. National strategies should not only protect agricultural land in Java but also establish new agricultural zones outside the island to ensure food security and self-sufficiency. In Cilegon, the observed land cover changes were consistent with the City's Spatial Plan, suggesting compatibility between current urban expansion and existing planning frameworks. Future applications should integrate high-resolution imagery (e.g., Sentinel-2) and advanced classification algorithms, particularly in heterogeneous landscapes where mixed pixels are prevalent. Combining Landsat with higher-resolution datasets would enhance classification accuracy and policy relevance in rapidly urbanizing areas. Incorporating socio-economic and demographic datasets into spatial analysis would further enable comprehensive scenario modelling, allowing policymakers to anticipate land-use conflicts and design proactive mitigation strategies. Such outputs could directly support local governments, urban planners, and environmental agencies in zoning, agricultural land preservation, and targeted restoration programs to mitigate land degradation.

Acknowledgement

The authors gratefully acknowledge the local government of Cilegon City for providing statistical data, as well as USGS and NASA for freely providing Landsat-5 TM and Landsat-9 OLI-2 imagery.

Author Contributions

Riska Ayu Purnamasari: Methodology, formal analysis, writing - reviewing and editing, and funding acquisition. Marwan Setiawan: Data Visualization, Wardah Wardah: Supervision.

Funding Sources

This research received no specific grant from funding agencies in the public, commercial, or not-for-profit sectors.

Competing Interest

The authors declare that they have no known competing financial interests or personal relationships that could have appeared to influence the work reported in this paper.

References

[1] Smith, P.; Gregory, P. J.; Van Vuuren, D.; Obersteiner, M.; Havlík, P.; Rounsevell, M.; Bellarby, J. (2010). Competition for land. *Philosophical Transactions of the Royal Society B: Biological Sciences*, *365*(1554), 2941–2957. https://doi.org/10.1098/rstb.2010.0127.

[2] Xiao, Y.; Mignolet, C.; Mari, J. F.; Benoît, M. (2014). Modeling the spatial distribution of crop sequences at a large regional scale using land-cover survey data: A case from France. *Computers and Electronics in Agriculture*, *102*, 51–63. https://doi.org/10.1016/j.compag.2014.01.010.

[3] Haberl, H. (2015). Competition for land: A sociometabolic perspective. *Ecological Economics*, *119*, 424–431. https://doi.org/10.1016/j.ecolecon.2014.10.002.

[4] Hatab, A. A.; Cavinato, M. E. R.; Lindemer, A.; Lagerkvist, C. J. (2019). Urban sprawl, food security and agricultural systems in developing countries: A systematic review of the literature. *Cities*, *94*, 129–142. https://doi.org/10.1016/j.cities.2019.06.001.

[5] Wu, K. Y.; Ye, X. Y.; Qi, Z. F.; Zhang, H. (2013). Impacts of land use/land cover change and socioeconomic development on regional ecosystem services: The case of fast-growing Hangzhou metropolitan area, China. *Cities*, *31*, 276–284. https://doi.org/10.1016/j.cities.2012.08.003.

[6] Altieri, M. A.; Companioni, N.; Cañizares, K.; Murphy, C.; Rosset, P.; Bourque, M.; Nicholls, C. I. (1999). The greening of the "barrios": Urban agriculture for food security in Cuba. *Agriculture and Human Values*, *16*, 131–140. https://doi.org/10.1023/A:1007545304561.

[7] Zezza, A.; Tasciotti, L. (2010). Urban agriculture, poverty, and food security: Empirical evidence from a sample of developing countries. *Food Policy*, *35*(4), 265–273. https://doi.org/10.1016/j.foodpol.2010.04.007.

[8] Satterthwaite, D.; McGranahan, G.; Tacoli, C. (2010). Urbanization and its implications for food and farming. *Philosophical Transactions of the Royal Society B: Biological Sciences*, *365*(1554), 2809–2820. https://doi.org/10.1098/rstb.2010.0136.

[9] Harini, R.; Yunus, H. S.; Kasto; Hartono, S. (2012). Agricultural land conversion: determinants and impact for food sufficiency in Sleman regency. *Indonesian Journal of Geography*, *44*(2), 120–133.

[10] Bajocco, S.; Smiraglia, D.; Scaglione, M.; Raparelli, E.; Salvati, L. (2018). Exploring the role of land degradation on agricultural land use change dynamics. *Science of the Total Environment*, *636*, 1373–1381. https://doi.org/10.1016/j.scitotenv.2018.05.119.

[11] Firman, T. (2017). The urbanization of Java, 2000–2010: Towards 'the island of mega-urban regions. *Asian Population Studies*, *13*(1), 50–66. https://doi.org/10.1080/17441730.2016.1247587.

[12] Doydee, P. (2005). Coastal landuse change detection using remote sensing technique: Case study in Banten Bay, West Java Island, Indonesia. *Agriculture and Natural Resources*, *39*(1), 159–164. https://li01.tci-thaijo.org/index.php/anres/article/view/243296.

[13] Tassi, A.; Massetti, A.; Gil, A. (2022). The spectralrao-monitoring Python package: A RAO's Q diversity index-based application for land-cover/land-use change detection in multifunctional agricultural areas. *Computers and Electronics in Agriculture*, *196*, 106861. https://doi.org/10.1016/j.compag.2022.106861.

[14] da Silveira, F.; Lermen, F. H.; Amaral, F. G. (2021). An overview of agriculture 4.0 development: Systematic review of descriptions, technologies, barriers, advantages, and disadvantages. *Computers and Electronics in Agriculture*, *189*, 106405. https://doi.org/10.1016/j.compag.2021.106405.

[15] Gandharum, L.; Mulyani, M. E.; Hartono, D. M.; Karsidi, A.; Ahmad, M. (2021). Remote sensing versus the area sampling frame method in paddy rice acreage estimation in Indramayu regency, West Java province, Indonesia. *International Journal of Remote Sensing*, *42*(5), 1738–1767. https://doi.org/10.1080/01431161.2020.1842541.

[16] Purnamasari, R. A.; Noguchi, R.; Ahamed, T. (2019). Land suitability assessments for yield prediction of cassava using geospatial fuzzy expert systems and remote sensing. *Computers and Electronics in Agriculture*, *166*, 105018. https://doi.org/10.1016/j.compag.2019.105018.

[17] Lobell, D. B.; Thau, D.; Seifert, C.; Engle, E.; Little, B. (2015). A scalable satellite-based crop yield mapper. *Remote Sensing of Environment*, *164*, 324–333. https://doi.org/10.1016/j.rse.2015.04.021.

[18] Guan, K.; Li, Z.; Rao, L. N.; Gao, F.; Xie, D.; Hien, N. T.; Zeng, Z. (2018). Mapping paddy rice area and yields over Thai Binh Province in Viet Nam from MODIS, Landsat, and ALOS-2/PALSAR-2. *IEEE Journal of Selected Topics in Applied Earth Observations and Remote Sensing*, *11*(7), 2238–2252. https://doi.org/10.1109/JSTARS.2018.2834383.

[19] Forkuor, G.; Dimobe, K.; Serme, I.; Tondoh, J. E. (2018). Landsat-8 vs. Sentinel-2: Examining the added value of sentinel-2's red-edge bands to land-use and land-cover mapping in Burkina Faso. *GIScience & Remote Sensing*, *55*(3), 331–354. https://doi.org/10.1080/15481603.2017.1370169.

[20] Arekhi, M.; Goksel, C.; Balik Sanli, F.; Senel, G. (2019). Comparative evaluation of the spectral and spatial consistency of Sentinel-2 and Landsat-8 OLI data for Igneada longos forest. *ISPRS International Journal of Geo-Information*, *8*(2), 56. https://doi.org/10.3390/ijgi8020056.

[21] Dornik, A.; Cheţan, M. A.; Drăguţ, L.; Iliuţă, A.; Dicu, D. D. (2022). Importance of the mapping unit on the land suitability assessment for agriculture. *Computers and Electronics in Agriculture*, *201*, 107305. https://doi.org/10.1016/j.compag.2022.107305.

[22] Hussain, M.; Chen, D.; Cheng, A.; Wei, H.; Stanley, D. (2013). Change detection from remotely sensed images: From pixel-based to object-based approaches. *ISPRS Journal of Photogrammetry and Remote Sensing*, *80*, 91–106. https://doi.org/10.1016/j.isprsjprs.2013.03.006.

[23] Jiang, D.; Huang, Y.; Zhuang, D.; Zhu, Y.; Xu, X.; Ren, H. (2012). A simple semi-automatic approach for land cover classification from multispectral remote sensing imagery. *PLoS One*, *7*(9), e45889. https://doi.org/10.1371/journal.pone.0045889.

[24] Arvor, D.; Betbeder, J.; Daher, F. R.; Blossier, T.; Le Roux, R.; Corgne, S.; da Silva Junior, C. A. (2021). Towards user-adaptive remote sensing: Knowledge-driven automatic classification of Sentinel-2 time series. *Remote Sensing of Environment*, *264*, 112615. https://doi.org/10.1016/j.rse.2021.112615.

[25] García-Álvarez, D.; Camacho Olmedo, M. T.; Paegelow, M.; Mas, J. F. (2022). Land use cover datasets and validation tools: Validation practices with QGIS. *Lecture Notes in Geoinformation and Cartography*, Springer, Cham. https://doi.org/10.1007/978-3-030-90998-7.

[26] Yuh, Y. G.; Tracz, W.; Matthews, H. D.; Turner, S. E. (2023). Application of machine learning approaches for land cover monitoring in northern Cameroon. *Ecological Informatics*, *74*, 101955. https://doi.org/10.1016/j.ecoinf.2022.101955.

[27] Olofsson, P.; Foody, G. M.; Herold, M.; Stehman, S. V.; Woodcock, C. E.; Wulder, M. A. (2014). Good practices for estimating area and assessing the accuracy of land change. *Remote Sensing of Environment*, *148*, 42–57. https://doi.org/10.1016/j.rse.2014.02.015.

[28] Yahaya, T. O.; Salisu, T. F.; Yunusa, A.; John, E.; Yusuf, A. B.; Umar, A. K.; Abe, O. (2023). Assessment of anthropogenic impact on ecosystem service safety of Agboyi River in Lagos,

Southwestern, Nigeria. *Tropical Aquatic and Soil Pollution*, *3*(2), 184–195. https://doi.org/10.53623/tasp.v3i2.281.

[29] Gandharum, L.; Hartono, D. M.; Karsidi, A.; Ahmad, M. (2022). Monitoring urban expansion and loss of agriculture on the north coast of West Java province, Indonesia, using Google Earth Engine and intensity analysis. *The Scientific World Journal*, *2022*(1), 3123788. https://doi.org/10.1155/2022/3123788.

[30] Gandharum, L.; Hartono, D. M.; Karsidi, A.; Ahmad, M.; Prihanto, Y.; Mulyono, S.; Alhasanah, F. (2024). Past and future land use change dynamics: Assessing the impact of urban development on agricultural land in the Pantura Jabar region, Indonesia. *Environmental Monitoring and Assessment*, *196*(7), 645. https://doi.org/10.1007/s10661-024-12889-3.